引用格式：XU Geliang，XU Jian，KONG Lingli，et al. Reconfigurable Optical Chaotic Logic Operations with Fast Rate of Picoseconds Scale[J]. Acta Photonica Sinica，2021，50(5)：0506008
许葛亮，徐健，孔令立，等.皮秒量级的快速率可重构光混沌逻辑运算[J].光子学报，2021，50(5)：0506008

皮秒量级的快速率可重构光混沌逻辑运算

许葛亮，徐健，孔令立，黄其锋，仇显婷，郭洋洋，程峰
（巢湖学院 电子工程学院，合肥 238000）

摘 要：基于垂直腔表面发射激光器（VCSEL）自身的光反馈以及线性电光调制效应，设计了一种实现动态可重构的光混沌逻辑运算的技术方案。归一化注入电流被调制为逻辑输入，横向电场被调制为控制信号，逻辑输出通过对VCSEL输出的x偏振光光强的均值与阈值做差进行解调。通过转换控制信号与逻辑输入的逻辑运算关系，系统就能在基本的逻辑运算如NOT、AND、NAND、OR、NOR、XOR以及XNOR间自由切换。码元宽度为600 ps且噪声强度高达2.75×10^9情况下，逻辑运算的成功概率仍为1，表明系统具有良好的抗噪声性能。并且噪声强度等于2.5×10^9时，码元宽度至少达到579 ps，逻辑运算的成功概率才恒为1。本文研究对于研发快速稳定的组合逻辑运算器件等具有参考价值。

关键词：垂直腔表面发射激光器；可重构；光混沌逻辑运算；皮秒量级
中图分类号：N93 **文献标识码**：A **doi**：10.3788/gzxb20215005.0506008

Reconfigurable Optical Chaotic Logic Operations with Fast Rate of Picoseconds Scale

XU Geliang，XU Jian，KONG Lingli，HUANG Qifeng，QIU Xianting，GUO Yangyang，CHENG Feng
（*School of Electronic Engineering*，*Chaohu University*，*Hefei* 238000，*China*）

Abstract：In order to realize dynamic and reconfigurable optical chaotic logic operations，a specific technical scheme based on Vertical Cavity Surface Emitting Laser（VCSEL）feedback by its own light and linear electro-optic modulation effect has been proposed. The normalized injection current is modulated as logic input，the transverse electric field is modulated as control signal，and the logic output is demodulated by the difference between the average value and the threshold value of the x-polarized light intensity from the output of VCSEL. By transforming the logic operation relationship between control signal and logic input，the system can switch freely among basic logic operations such as NOT，AND，NAND，OR，NOR，XOR and XNOR. When the code width is 600 ps and the noise intensity is as high as 2.75×10^9，the success probability of the logic operation still equals 1，indicating that the system has good anti-noise performance. And when the noise intensity equals 2.5×10^9，the success probability always equals 1 if the code width is at least 579 ps. The above results have great reference value for the development of fast and

Foundation item：Natural Science Foundation of the Higher Education Institutions of Anhui Province（No. KJ2019A0685），the School-Level Scientific Research Project of Chaohu University（No. XLY-202001），the National College Students Innovation and Entrepreneurship Training Program of Chaohu University in 2019（No. 201910380019），the National College Students Innovation and Entrepreneurship Training Program of Chaohu University in 2020（No. 202010380011）
First author：XU Geliang（1991—），male，assistant professor，M.S. degree，mainly focuses on chaotic laser communication and nonlinear optics. Email：xugeliang1027@163.com
Contact author：KONG Lingli（1988—），male，lecturer，Ph.D. degree，mainly focuses on signal processing and photoelectric detection. Email：948978802@qq.com
Received：Jan. 6，2021；**Accepted**：Feb.22，2021

stable combinational logic operation devices.

Key words: Vertical Cavity Surface Emitting Laser (VCSEL); Reconfigurable; Optical chaotic logic operation; Picoseconds scale

OCIS Codes: 060.4510; 140.1540; 140.3460; 140.3510

0 Introduction

With the rapid development of communication technology, optical communication has been widely used in the market because of its large communication capacity, low transmission loss and large frequency bandwidth. The chaotic laser signal, which is highly sensitive to the initial conditions of the system and external interference, has strong randomness and is not easy to be deciphered. So now which it has been widely used in the field of secure optical communication. Meanwhile, the logic operations realized by chaotic signals generated by semiconductor lasers have attracted great attention currently. Compared with edge-emitting laser, Vertical Cavity Surface Emitting Laser (VCSEL) has the advantages of low production cost, small divergence angle, small size and low threshold current [1-6], etc. In addition, it can excite mutually orthogonal chaotic x-Polarized Light (x-PL) and chaotic y-Polarized Light (y-PL) under current or feedback injection of external light. The polarization switching and bistability can also be induced under suitable parameter conditions [7-11]. Based on VCSEL′s nonlinear dynamics, previous work has exploited different experimental schemes to realize optical logic gates. Based on polarization bistability, noise and tunable light injection, Masoller *et al* explored experimental schemes for random logic gate and all-optical logic gate [12-14]. For laser amplitude modulation based on coupled feedback and parallel synchronization of laser chaos, Yan realized photoelectric composite logic gate and all-optical logic gate [3-4]. In 2015, our research group reported the experimental scheme of optoelectronic composite logic gate based on polarization switching in Optics Express [10]. In 2016, based on the generalized chaos synchronization theory and the polarization switching, we also realized the all-optical random logic gate [15]. In 2017, using frequency detuning to control polarization bistability, we further obtained dynamic all-optical chaotic logic operations [16].

Most of the above solutions implemented static logic operations. In the past, our research group studied logic operations with code width of 10ns (the operation rate is 0.1 GHz) [16], the operation rate needs to be improved. Here in the paper, based on the theory of linear electro-optic modulation, reconfigurable chaotic logic operations with fast rate and good anti-noise performance are realized by the scheme of VCSEL feedback by its own light in this paper. The second part below describes the basic theory and model in detail, the third part shows the experimental results and discussion, and the fourth part is the conclusions.

1 Theory and model

The system composition and detailed light path are shown in Fig. 1. Here, the normalized injection current μ is the sum of two square waves of $d\mu_1$ and $d\mu_2$ that encode two logic inputs I_1 and I_2, i.e., $\mu = d\mu_1(I_1) + d\mu_2(I_2)$. The transverse electric field E_0 is represented by a square wave that encode the control signal L_c, the high level and low level of the square wave are represented by E_{02} and E_{01} respectively. When $E_0 = E_{01}$, $L_c = 0$; and $L_c = 1$ if $E_0 = E_{02}$. Supposing that the average value of x-PL intensity from the VCSEL defined as A, its threshold is fixed at A^*. The steps of realizing reconfigurable chaotic logic operations are as follows

1) The appropriate values for normalized injection current $\mu(t)$ [$d\mu_1(t)$, $d\mu_2(t)$] and transverse electric field $E_0(t)$ are selected to encode the logic inputs [$I_1(t)$, $I_2(t)$] and control signal $L_c(t)$;

2) Add the normalized injection current and control signal, $I(t) = I_1(t) + I_2(t)$ and $L_c(t)$;

3) Use an electronic logic calculator to make $L_c(t)$ and $I_1(t)$ and $I_2(t)$ satisfying different logic operation relationships such as NOT, AND, NAND, OR, NOR, XOR and XNOR in different time periods; for the logic NOT operation, $I_1(t) = I_2(t)$.

4) Calculate the average value A under each group of logic inputs.

5) Threshold mechanism for obtaining the logic output, i.e., with the fixed threshold A^*, the logic out $X_o = 0$ if $A - A^* \leqslant 0$; $X_o = 1$ if $A - A^* > 0$.

Next, the working principle of the system is presented. The light emitted by VCSEL passes through the

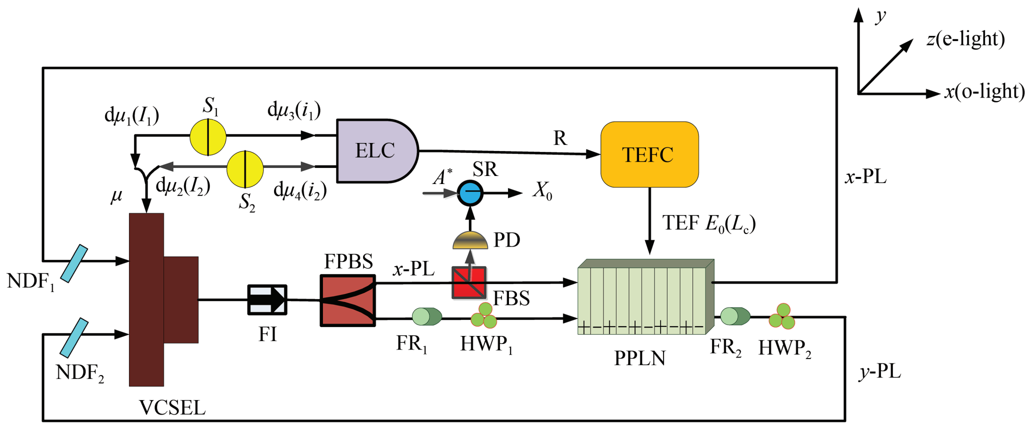

Fig. 1 Schematic diagram for reconfigurable chaotic logic operations of VCSEL with optical feedback

Fiber Isolator (FI) and then is separated by the Fiber Polarization Beam Splitter (FPBS) into x-PL and y-PL. The x-PL is split into two beams by a Fiber Splitter (FPS), one of which is converted into an electric signal by Photodetector (PD). The electric signal is used to demodulate the logic output through Subtracter (SR). Another x-PL beam is directly injected into the PPLN crystal as o-light input. The y-PL converts the polarized direction to the direction of the z-axis of the crystal by Faraday Rotator 1 (FR_1) and Half-Wave Plate 1 (HWP_1), and then injects into crystal as e-light input. After linear electro-optic modulation, the x-PL output from the PPLN crystal passes through the Neutral Density Filter 1 (NDF_1), and the y-PL passes through FR_2, HWP_2, and NDF_2. Then they are feedback into the VCSEL together. The feedback delay is τ, and NDF_1 and NDF_2 are used to control the feedback strength of x-PL and y-PL respectively.

In order to realize dynamic and reconfigurable chaotic logic operations, it is necessary for the control signal to change synchronously with the logic inputs. To solve this problem, we propose the following scheme: since the normalized injection current $\mu = \mathrm{d}\mu_1 + \mathrm{d}\mu_2$, and $\mathrm{d}\mu_1$ and $\mathrm{d}\mu_2$ are encoded into two logic inputs I_1 and I_2 respectively. Here we use time-varying current source S_1 to generate two identical electrical signals $\mathrm{d}\mu_1$ and $\mathrm{d}\mu_3$. Similarly, the same two electrical signals $\mathrm{d}\mu_2$ and $\mathrm{d}\mu_4$ are generated by S_2. And $\mathrm{d}\mu_3$ and $\mathrm{d}\mu_4$, in turn, are encoded into two electric logic inputs of Electronic Logic Calculator (ELC) such as $i_1$and i_3. Due to $\mathrm{d}\mu_1 = \mathrm{d}\mu_3$ and $\mathrm{d}\mu_2 = \mathrm{d}\mu_4$, the logic sets of the signals i_1 and i_2 are synchronized with those of the signals I_1 and I_2. The logic output of the ELC is defined as R, which can control the Transverse Electric Field (TEF) E_0 by Transverse Electric Field Controller (TEFC). Here, $R=0$ is encoded in the low level E_{01}, $R=1$ is encoded in the high level E_{02}. If $R=0$, we obtain $E_0 = E_{01}$ and $L_c = 0$; when $R=1$, we have $E_0 = E_{02}$ and $L_c = 1$. Using the ELC, R and i_1, i_2 can perform different logic operations, so that L_c can implement different logic operations with I_1 and I_2 indirectly. It is noted that the switching rate of the control signal is determined by ELC. At present, the reconfigurable operation rate of ELC can reach more than 10 GHz, which can satisfy the needs of reconfigurable chaotic logic operations realized in this paper.

Due to the VCSEL subject to the delay feedback of its own light, the dynamic equations of x-PL and y-PL are represented as follows

$$\frac{\mathrm{d}}{\mathrm{d}t}\begin{pmatrix} E_x(t) \\ E_y(t) \end{pmatrix} = k(1+\mathrm{i}a)\{[N(t)-1]\}\begin{pmatrix} E_x(t) \\ E_y(t) \end{pmatrix} \pm k(1+\mathrm{i}a)\mathrm{i}n(t)\begin{pmatrix} E_y(t) \\ E_x(t) \end{pmatrix} \mp (\gamma_a + \mathrm{i}\gamma_p)\begin{pmatrix} E_x(t) \\ E_y(t) \end{pmatrix} + k_f\begin{pmatrix} E_x(t-\tau) \\ E_y(t-\tau) \end{pmatrix} \times \exp(-\mathrm{i}\omega_0\tau) + \begin{pmatrix} \sqrt{\beta_{sp}\gamma_e N}\,\zeta_x \\ \sqrt{\beta_{sp}\gamma_e N}\,\zeta_y \end{pmatrix} \tag{1}$$

$$\frac{\mathrm{d}N(t)}{\mathrm{d}t} = -\gamma_e\{N(t) - \mu + N(t)(|E_x(t)|^2 + |E_y(t)|^2) + \mathrm{i}n(t)[E_y(t)E_x^*(t) - E_x(t)E_y^*(t)]\} \tag{2}$$

$$\frac{\mathrm{d}n(t)}{\mathrm{d}t} = -\gamma_s n(t) - \gamma_e\{n(t)(|E_x(t)|^2 + |E_y(t)|^2) + \mathrm{i}N(t)[E_y(t)E_x^*(t) - E_x(t)E_y^*(t)]\} \tag{3}$$

In the above formulas, subscripts x and y mean x-PL and y-PL respectively; E represents the complex amplitude of light; N is the total carrier concentration; n is the difference in concentration between carriers with spin-up and carriers with spin-down; ω_0 is the center frequency of light; β_{sp} represents the spontaneous emission factor, which is also defined as noise intensity; ζ_x and ζ_y are a pair of gaussian white noises that are independent of each other and obey the standard normal distribution. The meanings and values of other physical quantities are shown in Table 1 below.

Table 1 The main parameters of the system

Parameter and symbol	Value	Parameter and symbol	value
Line-width enhancement factor a	3	Duty ratio R	0.5
field decay rate k	300	Polar angle θ/π	1/2
Spin relaxation rate $\gamma_s/\mathrm{ns}^{-1}$	50	Azimuth φ	0
Nonradiative carrier relaxation $\gamma_e/\mathrm{ns}^{-1}$	1	Crystal temperature F/ K	293
Dichroism $\gamma_a/\mathrm{ns}^{-1}$	−0.1	Poled period of crystal Λ/m^{-1}	5.8×10^5
Birefringence $\gamma_p/\mathrm{ns}^{-1}$	2	Crystal length L/mm	15
Delay time τ/ns	2	Refractive index of o-light n_1	2.24
Effective refractive index of active layer n_g	3.6	Refractive index of e-light n_2	2.17
Effective area of light spot $S_A/\mu\mathrm{m}^2$	38.485	Differential material gain g/ $\mathrm{m^3 \cdot s^{-1}}$	2.9×10^{-12}
Length of the laser cavity $L_v/\mu\mathrm{m}$	10	Field confinement factor to the active region Γ	0.05
Optical feedback strength k_f	1.13	Volume of the active layer $V/\mu\mathrm{m}^3$	384.85
Code width T/ps	600	The noise intensity β_{sp}	2.5×10^9

The x-PL and y-PL from VCSEL are injected into the PPLN crystal and converted into o-light and e-light respectively, and their amplitudes satisfy the following relationship

$$U_{x,y}(0,t-\tau)=\sqrt{\frac{\hbar\omega_0 V}{S_A T_L v_c n_{1,2}}}E_{x,y}(t-\tau) \tag{4}$$

The linear EO modulation effect occurs in the PPLN crystal, and coupled wave equation of o-light and e-light can be expressed as follows

$$U_{x,y}(L,t-\tau)=\rho_{x,y}(L,t-\tau)\exp(\mathrm{i}\beta_0 L)\exp\left[\mathrm{i}\phi_{x,y}(L,t-\tau)\right] \tag{5}$$

where

$$\rho_{x,y}(L,t-\tau)=\left\{U_{x,y}^2(0,t-\tau)\cos^2(vL)+\left[\frac{\gamma U_{x,y}(0,t-\tau)\mp d_{1,3}U_{y,x}(0,t-\tau)}{v}\right]^2\sin^2(vL)\right\}^{1/2} \tag{6}$$

$$\phi_{x,y}(L,t-\tau)=\arctan\left[\frac{\pm\gamma U_{x,y}(0,t-\tau)-d_{1,3}U_{y,x}(0,t-\tau)}{vU_{x,y}(0,t-\tau)}\tan(vL)\right] \tag{7}$$

$$\beta_0=\frac{\Delta k-d_2-d_4}{2} \tag{8}$$

and

$$v=\sqrt{\frac{(\Delta k+d_2-d_4)^2+4d_1d_3}{2}} \tag{9}$$

$$\gamma=\frac{d_4-d_2-\Delta k}{2} \tag{10}$$

U_x and U_y in Eqs. (4)~(10) represent the amplitudes of o-light and e-light respectively; T_L represents the time it takes for light to travel back and forth in the laser cavity once; $\hbar$ is the Planck constant; $\Delta k=k_x-k_y+K_1$, k_x and k_y denote the wave vectors of o-light and e-light at ω_0, and $k_x=2\pi n_1 v_c/\omega_0$, $k_y=2\pi n_2 v_c/\omega_0$, $K_1=2\pi/\Lambda$, Λ is the poled period, where the coefficients d_1, d_2, d_3, and d_4 are presented in Ref.[17]. The meanings and values of other physical quantities are presented in Table 1. The o-light and e-light are converted into x-PL and y-PL respectively after being output from the crystal, and the conversion relationship can be expressed as follows

$$E_{x,y}(t-\tau)=\sqrt{\frac{S_A T_L v_c n_{1,2}}{\hbar\omega_0 V}}U_{x,y}(L,t-\tau) \tag{11}$$

2 Results and discussions

The Eqs. (1)～(3) can be solved according to the fourth-order Runge-Kutta method and the system parameters in Table 1. Because $\mu=\mathrm{d}\mu_1+\mathrm{d}\mu_2$, $\mathrm{d}\mu_1$ and $\mathrm{d}\mu_2$ are used to modulate binary logic inputs I_1 and I_2, respectively. The logic input sequence (I_1, I_2) has four combinations as (0, 0), (0, 1), (1, 0) and (1, 1), and the specific modulation rules are: when $\mathrm{d}\mu_1=0.74$, $I_1=0$, and when $\mathrm{d}\mu_1=0.75$, $I_1=1$. Similarly, when $\mathrm{d}\mu_2=0.74$, $I_2=0$; when $\mathrm{d}\mu_2=0.75$, $I_2=1$. Therefore, when logic input $(I_1, I_2)=(0, 0)$, $\mu=\mathrm{d}\mu_1+\mathrm{d}\mu_2=1.48$; while $(I_1, I_2)=(0, 1)$ or $(1, 0)$, $\mu=\mathrm{d}\mu_1+\mathrm{d}\mu_2=1.49$; and $\mu=\mathrm{d}\mu_1+\mathrm{d}\mu_2=1.50$ if logic input $(I_1, I_2)=(1, 1)$. The control signal L_c is modulated by the transverse electric field E_0, it means that, if $E_0=E_{02}=0.75$ kV/mm, $L_c=1$; else if $E_0=E_{01}=0.589\ 4$ kV/mm, $L_c=0$. Moreover, the logic output X_o can be demodulated by performing difference processing between A and the threshold $A*$ under each logic input, namely, if $A\leqslant A^*$, $X_o=0$, else if $A>A^*$, $X_o=1$.

The threshold value A^* determines the reliability of the logic operations. In order to obtain a suitable threshold, we adopt the following technical solutions: since L_c and (I_1, I_2) can form the basic logic operation relationships such as NOT, AND, OR, XOR, etc., for each of the above-mentioned logic operation relations, we have calculated the maximum average A_{max} of x-PL intensity when $L_c=0$, and the minimum average A_{min} under $L_c=1$, as shown in Table 2. It can be found from the table that in all the logic relationships that L_c and (I_1, I_2) satisfy, the maximum value of A when $L_c=0$ is $A_{max}=0.003$, and that's minimum value when $L_c=1$ is $A_{min}=0.021$. Therefore, the threshold A^* must meet $0.003<A^*<0.021$. Here we take $A*=0.013$, that is, if $A\leqslant 0.013$, $X_o=0$; otherwise $X_o=1$.

Table 2 For the different logic operations relationship between L_c and (I_1, I_2), the maximum average (A_{max}) of the x-PL intensity under L_c=0 and its minimum average (A_{min}) under L_c=1.

Logic operations	$(I_1, I_2)=(0, 0)$		$(I_1, I_2)=(0, 1)/(1, 0)$		$(I_1, I_2)=(1, 1)$	
	L_c	A	L_c	A	L_c	A
$L_c=I_1\cdot I_2$	0	$A_{max}=0$	0	$A_{max}=0$	1	$A_{min}=0.021$
$L_c=\overline{I_1\cdot I_2}$	1	$A_{min}=0.031$	1	$A_{min}=0.027$	0	$A_{max}=0.0014$
$L_c=I_1+I_2$	0	$A_{max}=0.0014$	1	$A_{min}=0.03$	1	$A_{min}=0.026$
$L_c=\overline{I_1+I_2}$	1	$A_{min}=0.034$	0	$A_{max}=0$	0	$A_{max}=0$
$L_c=I_1\oplus I_2$	0	$A_{max}=0.003$	1	$A_{min}=0.03$	0	$A_{max}=0.002$
$L_c=I_1\odot I_2$	1	$A_{min}=0.022$	0	$A_{max}=0$	1	$A_{min}=0.048$
$L_c=\overline{I_1}\,(\overline{I_2})$	1	$A_{min}=0.026$	*	*	0	$A_{max}=0.002$

When L_c and logic input satisfy different logic operation relationships, the system can implement different logic operations. In order to obtain logic AND operation, L_c needs to satisfy the AND operation relationship with I_1 and I_2 as shown in Fig.2(a). The solid green line represents E_0, the red dotted line represents the μ, and the blue solid line in Fig. 2 (b) denotes x-PL intensity I_x. When (I_1, I_2) equals (0, 0), (0, 1), (1, 0), respectively, x-PL intensity I_x is very small, and $A_{max}=0< A^*$ (see Table 2), then $X_o=0$; when $(I_1, I_2)=(1, 1)$, x-PL intensity I_x gets large, and $A_{min}=0.021>A^*$ (see Table 2), thus $X_o=1$, so the logic output is produced by demodulation as shown in Fig.2(c). In summary, the system has performed logic AND operation, namely $X_o=I_1\cdot I_2$. In the same way, $L_c=\overline{I_1\cdot I_2}$ is satisfied in Fig.2(a), and the system realizes logic NAND operation as shown in Fig.2(b), (c). Table 3 is the truth table of AND and NAND.

Similarly, we further obtain OR, NOR, XNOR, XOR and NOT operations, as shown in Fig.3, 4 and 5. Table 4, 5 and 6 are the truth tables for the above five logic operations.

The above-mentioned logic operations are performed under the condition that the control signal L_c and the logic input (I_1, I_2) form the static logic operation relationship. In order to show the reconfigurable ability of the system, relying on ELC to convert the logic relationship between L_c and (I_1, I_2) as shown in Fig.5(a), during the time of 3 ns～4.8 ns, 4.8 ns～7.2 ns, 7.2 ns～9.6 ns, 9.6 ns～12 ns, 12 ns～14.4 ns, 14.4 ns～16.8 ns, 16.8 ns～17.4 ns, L_c and (I_1, I_2) in turn form logic OR, XOR, XNOR, AND, NOR, NAND and NOT relationship, the reconfigurable logic operations are obtained as shown in Fig.5(b), (c).

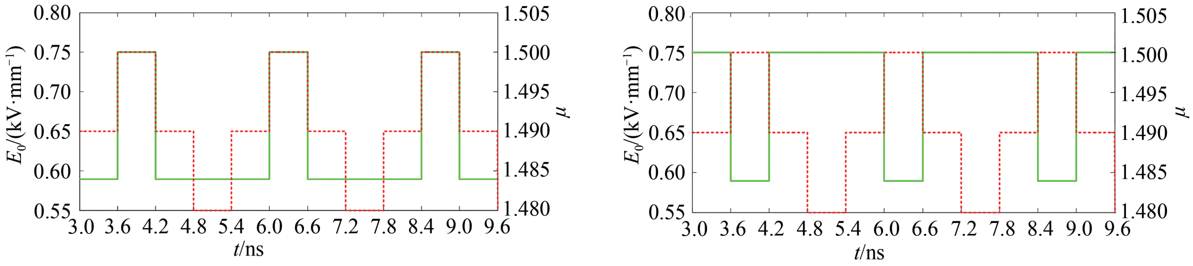

(a) The transverse electric field and normalized injection current

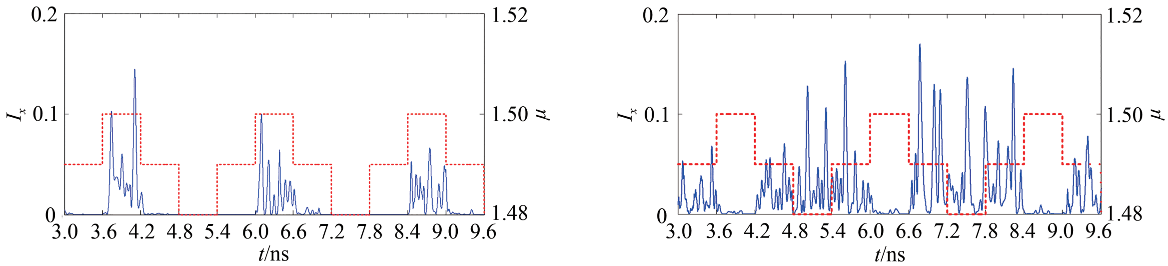

(b) The normalized injection current and intensity of x-PL

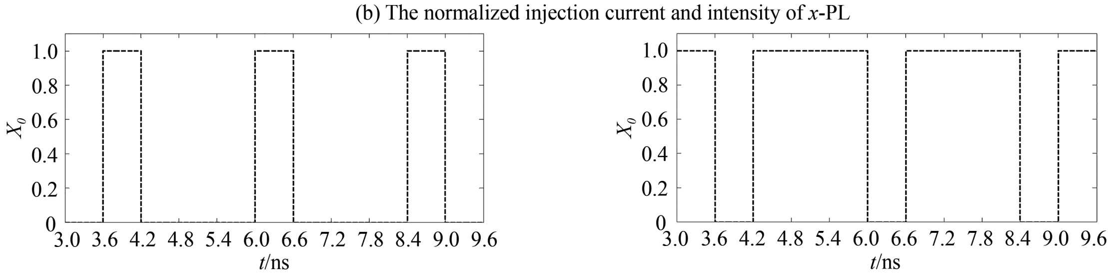

(c) The logic output

Fig. 2　The implementation of chaotic logic AND (left column) and NAND (right column) operations

Table 3　The truth table of logic AND and NAND

Logic input	AND		NAND	
(I_1, I_2)	L_c	X_o	L_c	X_o
(0,0)	0	0	1	1
(0,1)	0	0	1	1
(1,0)	0	0	1	1
(1,1)	1	1	0	0

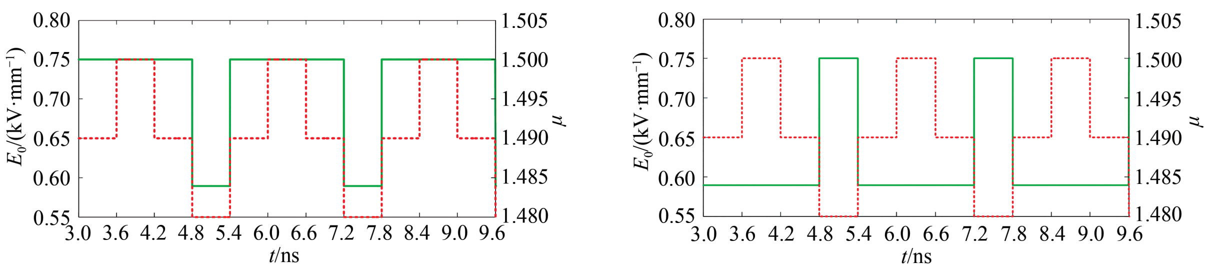

(a) The transverse electric field and normalized injection current

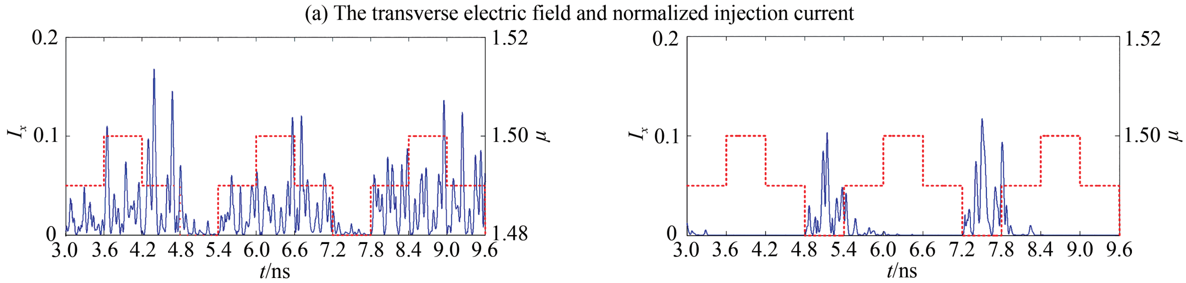

(b) The normalized injection current and the intensity of x-PL

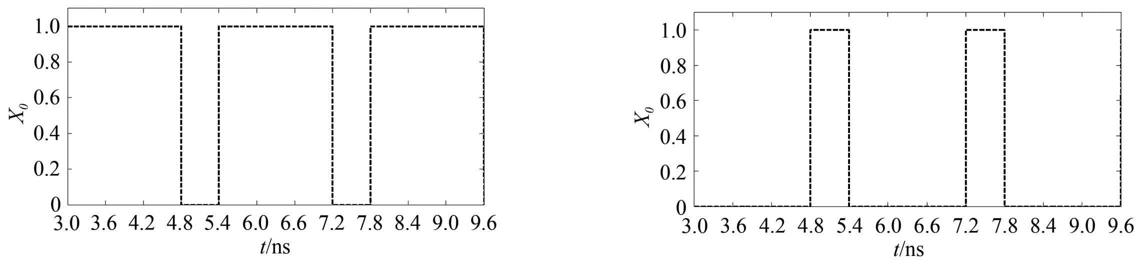

(c) The logic output

Fig. 3 The implementation of chaotic logic OR (left column) and NOR (right column) operations

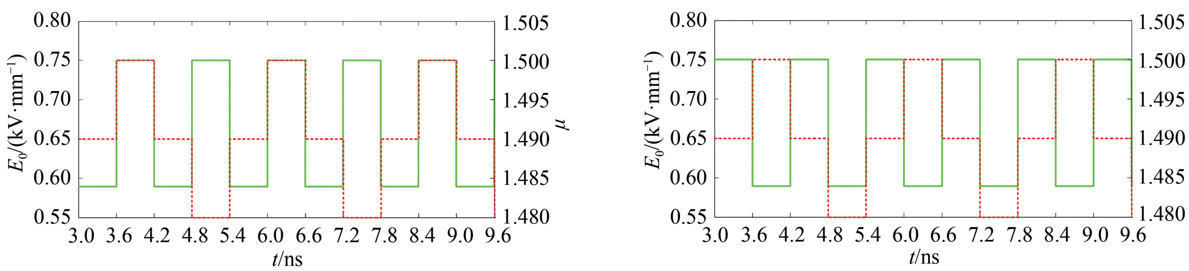

(a) The transverse electric field and normalized injection current

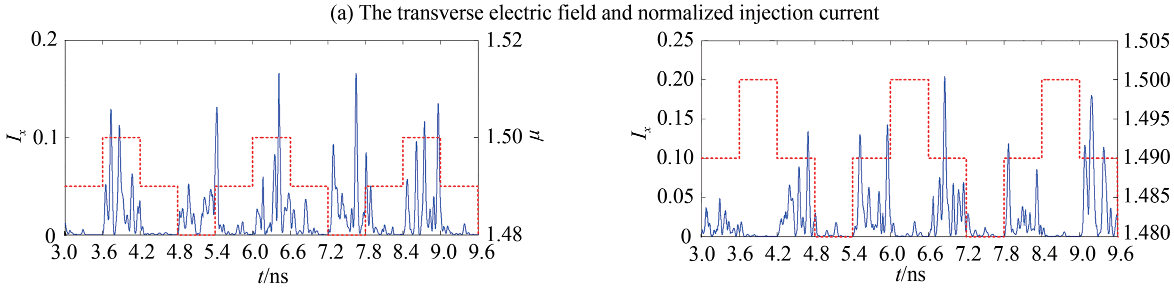

(b) The normalized injection current and the intensity of x-PL

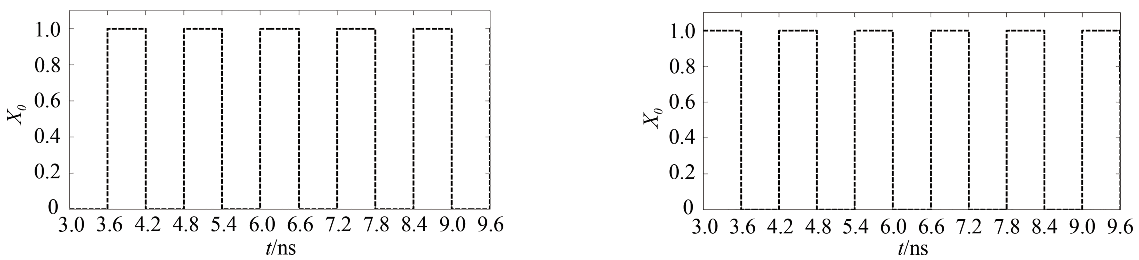

(c) The logic output

Fig. 4 The implementation of chaotic logic XNOR (left column) and XOR (right column) operations

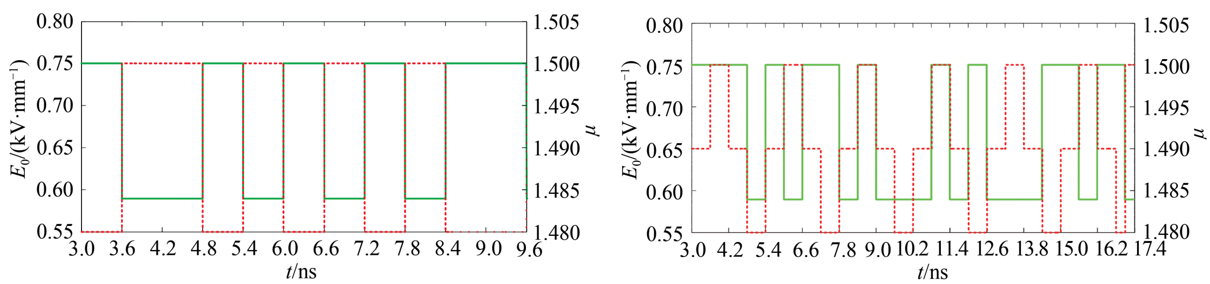

(a) The transverse electric field and normalized injection current

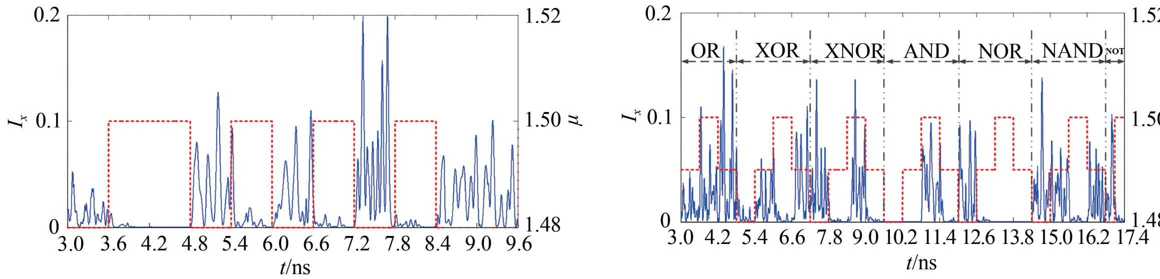

(b) The normalized injection current and the intensity of x-PL

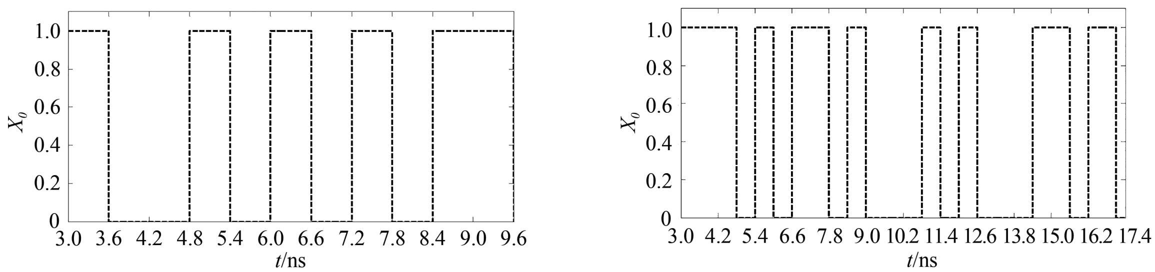

(c) The logic output

Fig. 5 The implementation of chaotic logic NOT (left column) and reconfigurable operations (right column)

Table 4 The truth table of logic OR and NOR

Logic input	OR		NOR	
(I_1, I_2)	L_c	X_o	L_c	X_o
(0,0)	0	0	1	1
(0,1)	1	1	0	0
(1,0)	1	1	0	0
(1,1)	1	1	0	0

Table 5 The truth table of logic XNOR and XOR

Logic input	XNOR		XOR	
(I_1, I_2)	L_c	X_o	L_c	X_o
(0,0)	1	1	0	0
(0,1)	0	0	1	1
(1,0)	0	0	1	1
(1,1)	1	1	0	0

Table 6 The truth table of logic NOT

Logic input	NOT	
(I_1, I_2)	L_c	X_o
(0,0)	1	1
(1,1)	0	0

The noise in the system has a significant impact on the reliability of logic operations [18]. Here, we introduce the success probability P to describe the reliability of the reconfigurable chaotic logic operations in Fig. 5(b). P is defined as the ratio between the number of the correct bits and that of total bits of the chaotic logic output. We calculate the dependence of the success probability P on the noise intensity β_{sp} as shown in Fig. 6. We can find that the value of P equals 1 when $\beta_{sp}<2.75\times10^9$. The value of P is greater than or equal to 0.92 even $2.75\times10^9<\beta_{sp}<4\times10^9$. These show that the reconfigurable optical chaotic logic operations have good anti-noise performance.

In order to explore the influence of code width T on the reliability of logic operations, we further calculate the dependence of the success probability P on the T as shown in Fig. 7. From the picture we can find that with the gradual increase of the T, the curve changes from violent oscillation to smaller fluctuation, and finally becomes a stable straight line with P always equals 1, which indicates that the larger the T, the better the reliability of the logic operations. We also discover the value of P equals 1 when T takes some values within 579 ps, such as T=104.5 ps, or T=107.9 ps, or T=124.8 ps, etc., but the value of P is unstable because a slight change in the value of T will cause the P to oscillate. And P always equals 1 when $T \geqslant 579$ ps. Therefore, reliable and stable logic operations can be obtained as long as the value of T is at least 579 ps.

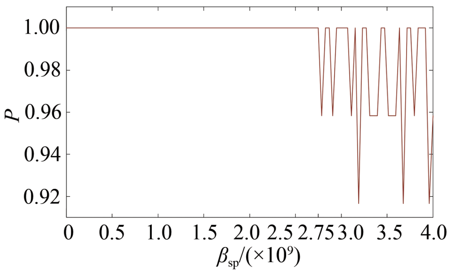

Fig. 6 The success probability of reconfigurable chaotic logic operations under different noise intensity

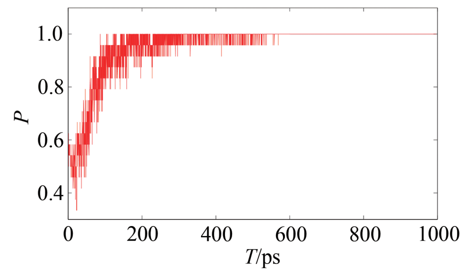

Fig. 7 The success probability of reconfigurable chaotic logic operation under different code width

3 Conclusions

Based on chaotic system of the VCSEL feedback by its own light and the linear electro-optic modulation effect, we have realized chaotic AND, OR, NOT, XOR, NAND, NOR and XNOR logic operations. The system can also perform reconfigurable logic operations by transforming the logic operation relationship between control signal and logic inputs. The further research shows that under code width T=600 ps, the success probability P always equals 1 when $\beta_{sp}<2.75\times 10^9$. The value of P is also greater than 0.92 even though $2.75\times 10^9<\beta_{sp}<4\times 10^9$. These results indicate that the reconfigurable chaotic logic operations have good anti-noise performance. Moreover, under $\beta_{sp}=2.5\times 10^9$, the value of P is unstable when T takes values within 579 ps. And the logic operations become reliable and stable as long as the value of T is at least 579 ps. The above research results have great application and reference value for the development of faster and safer combinatorial logic operation devices, such as optical full adders, optical data selectors, etc., as well as for the construction of reconfigurable optical networks.

References

[1] PERRONE S, VILASECA R, MASOLLER C. Stochastic logic gate that exploits noise and polarization bistability in an optically injected VCSEL[J]. Optics Express, 2012, 20(20): 22692-22699.

[2] ZHANG Xiaoxu, ZHANG Shenghai, WU Tianan, et al. Polarization switching characteristics of polarization maintaining optical feedback and orthogonal optical injection of 1550 nm-VCSEL[J]. Acta Physica Sinica, 2016, 65: 214206.

[3] YAN Senlin. Optoelectronic or all-optical logic gates using chaotic semiconductor lasers using mutual coupling-feedback [J]. Acta Physica Sinica, 2011, 65(21):214206.

[4] YAN Senlin. All-optical and combinational optoelectronic logic gates using chaotic synchronization of coupling-feedback semiconductor lasers and amplitude modulation[J]. Chinese Science Bulletin, 2011, 56(16): 1264-1271.

[5] YAN Senlin. Chaotic laser parallel synchronization and its application in all-optical logic gates[J]. Acta Physica Sinica, 2013, 62(23):230504.

[6] ZHONG Dongzhou, XIA Guangqiong, WANG Fei, et al. Vectorial chaotic synchronization characteristics of unidirectionally coupled and injected vertical-cavity surface-emitting lasers based on optical feedback[J]. Acta Physica Sinica, 2007, 56(6): 3279-3291.

[7] MARTIN-REGALADO J, PRATI F, MIGUEL M S, et al. Polarization properties of vertical-cavity surface emitting lasers[J]. IEEE Journal of Quantum Electronics, 1997, 3(2): 390-395.

[8] KAWAGUCHI H. Polarization-bistable vertical-cavity surface-emitting lasers: application for optical bit memory [J]. Opto-Electronics Review, 2009, 17(4): 265-274.

[9] KATAYAMA T, OOI T, KAWAGUCHI H. Experimental demonstration of multi-bit optical buffer memory using 1.55-um polarization bistable vertical cavity surface-emitting lasers[J]. IEEE Journal of Quantum Electronics, 2009, 45(11): 1495-1504.

[10] ZHONG Dongzhou, JI Yongqiang, LUO Wei. Controllable optoelectric composite logic gates based on the polarization switching in an optically injected VCSEL[J]. Optics Express, 2015, 23(23):29823-29833.

[11] QIU Haiying, WU Zhengmao, DENG Tao, et al. Polarization switching characteristics in a 1550 nm VCSEL subject to circularly polarized optical injection[J]. Chinese Optics Letters, 2016, 14(2):33-37.

[12] ZAMORA-MUNTAND J, MASOLLER C. Number implementation of a VCSEL-based stochastic logic gate via polarization bistability[J]. Optics Express, 2010, 18(16): 16418-16429.

[13] PERRONE S, VILASECA R, MASOLLER C. Stochastic logic gate that exploits noise and polarization bistability in an optically injected VCSEL[J]. Optics Express, 2012, 20(20): 22692-22699.

[14] SALVIDE M F, MASOLLER C, TORRE M S. All-optical stochastic logic gate based on a VCSEL with tunable optical injection[J]. IEEE Journal of Quantum Electronics, 2013, 49(10): 886 - 893.

[15] ZHONG Dongzhou, LUO Wei, XU Geliang . Controllable all-optical stochastic logic gates and their delay storages based on the cascaded VCSELs with optical-injection[J]. Chinese Physics B, 2016, 25(9): 094202.

[16] ZHONG Dongzhou, XU Geliang, LUO Wei. Reconfigurable dynamic all-optical chaotic logic operations in an optically injected VCSEL[J]. Chinese Physics B, 2017, 26(12): 261-271.

[17] LI Yan, WU Zhengmao, ZHONG Zhuqiang, et al. Time-delay signature of chaos in 1550nm VCSELs with variable-polarization FBG feedback[J]. Optics Express, 2014, 22(16): 19610-19620.

[18] ZHONG Dongzhou, YANG Guangze, XIAO Zhenzhen, et al. Optical chaotic data-selection logic operation with the fast response for picosecond magnitude[J]. Optics Express, 2019, 27(16): 23357-23367.